PERGAMON Journal of the Franklin Institute 336 (1999) 1225–1247

Journal
of The
Franklin Institute

www.elsevier.nl/locate/jfranklin

Bond graph-based simulation of non-linear inverse systems using physical performance specifications

Roger F. Ngwompo[a], Peter J. Gawthrop[b,*]

[a]*Department of Mechanical Engineering University of Bath, Bath BA2 7AY, England, UK*
[b]*Centre for Systems & Control and Department of Mechanical Engineering, University of Glasgow, Glasgow G12 8QQ, Scotland, UK*

Received 7 May 1998; received in revised form 9 September 1999

Abstract

Analysis and simulation of non-linear inverse systems are sometimes necessary in the design of control systems particularly when trying to determine an input control required to achieve some predefined output specifications. But unlike physical systems which are *proper*, the inverse systems are very often *improper* leading to numerical problems in simulation as their models sometimes have a high index when written in the form of differential-algebraic equations (DAE). This paper provides an alternative approach whereby performance specifications and the physical system are combined within a single bond graph leading to a greatly simplified simulation problem. © 2000 The Franklin Institute. Published by Elsevier Science Ltd. All rights reserved.

Keywords: Bond graphs; Inversion

1. Introduction

The modelling and simulation of physical systems (which are often non-linear) for analysis and evaluation of their dynamic behaviour are important steps in the design of control systems. As discussed previously [1,2], one such step is the choice of actuator appropriate for the control of a given system with a given output

* Corresponding author.
E-mail addresses: R.F.Ngwompo@bath.ac.uk (R.F. Ngwompo), P.Gawthrop@eng.gla.ac.uk (P.J. Gawthrop)

PII: S0016-0032(99)00032-0

performance specification, this will be called the *actuator sizing problem*. One possible approach is to successively design a controller, simulate it in closed loop, and extract the control signal information. However, this approach has the conceptual problem that actuator sizing is in fact independent of control law design and the practical problem that the control law must be designed first. In contrast, the inversion approach does *not* require prior control law design but rather gives the controller requirements (in terms of effort flow and power) in terms of system model and performance requirements.

In the case of linear systems, the fact that the transfer function of the inverse is improper has no severe conceptual and practical problem; but in the case of *non-linear* systems there are problems with this approach. In particular, the inversion approach has the problem that the resultant inverse model cannot be represented in the usual state-space form, but rather is a differential-algebraic equation (DAE). A DAE is associated with an *index* which "indicates the distance" between the set of differential and algebraic equations and the corresponding set of explicit ordinary differential equations that would be obtained through differential and algebraic operations on the original DAE model. The index determines the complexity or numerical difficulties in the integration of a differential-algebraic equation [3–5]. Index zero DAEs (which are ODEs) or index one DAEs can be handled by many DAE solvers using backward differentiation formulae (BDF) method providing that conditions for existence of a solution are satisfied. In the case of higher index DAEs, numerical methods are most of the time inefficient even if some models with special structures may be solved.

Although physical systems generally have an ordinary differential equation (or at least a low-index differential-algebraic equation) representation, an inverse system is usually a non-physically realizable system which will not admit a classical state space representation and its DAE model will have a high index depending on the input/output structure. Using a bond graph representation, it will be shown in Section 3 that this case of high index model is inherent to the nature of the inverse problem and there is no point to reconsider the model in order to lower the index as it was suggested for physical systems model. Moreover, except in some particular cases, symbolic transformations of the DAE model into an ODE form will not generally admit a classical state space representation as some derivatives of the inverse system input (which is the output of the forward system) usually appear in the ODE model. From these general observations, it then comes that simulation of inverse systems should be regarded in most cases either as simulation of high index models in DAE form or non-classical state-space models in ODE form and numerical integration methods are in general inefficient in dealing with such models. What can then be done to allow simulation software to deal with inverse models avoiding the need for DAE solvers?

This paper considers the problem of finding the system input (as a function of time) required to achieve a desired and predefined output specifications. Such specifications can be described in two ways:

(1) by explicitly defining an output trajectory (as a function of time);
(2) or by describing a reference model which specifies the performance of the actual system for a typical input.

In the first case, the prescribed output may not be realistic if it is defined without taking into account the capabilities of the actual system, for instance in terms of the smoothness of the given trajectory with respect to time. For example, it is obvious that the required output trajectory should be smooth enough according to the input–output relative degree. However, if the output trajectory is explicitly defined as an analytical function of time which is sufficiently differentiable, and if its required successive time-derivatives can be expressed analytically through symbolic differentiations, then the simulation of the inverse system may be considered using its ODE model which in this case is also called the minimal-order inverse model [6,7]. Unfortunately, successive time derivations and derivation of minimal-order inverse model are both often computationally inefficient.

The second case of performance specification via a reference system, if carried out properly in a physical model-based approach, has the advantage that it directly leads to a realistic output objective. Moreover, combining the physical specification model and the actual system in a certain configuration through their combined bond graph model allows determination of the input control required to achieve the output objective by simulating *proper or causal* system. Of course, as discussed in Section 4, the specification system must be chosen in such a way that its structure is such that the composite system is proper; but, as discussed in Section 4, this is easy to do using the physical model-based approach.

This paper focuses on the latter approach of physical performance specifications and the overall system configuration for simulation based on bond graph representation. In particular, the method is applicable to non-linear systems which may have an inverse of high order.

The aim of the paper is to find the control signal required to achieve a given performance specification *without the need to design a controller*; hence, the design of such a controller is a separate issue. However, some design methods are related to our approach. The "exact linearisation" approach [8], is one design method particularly relevant in this context in that it uses non-linear state-feedback to give a linear closed-loop system. The "exact linearisation" approach can be viewed as a non-linear version of linear model-following control (see, for example, Ref. [9] for a discussion). Model-predictive control provides a method for converting an open-loop control signal (such as that generated here) into a closed-loop controller. The state of the art in non-linear MPC is given in Ref. [10].

The outline of the paper is as follows: Section 2 recalls the concept and a procedure for system inversion using the bond graph representation and bicausality. Section 3 points out some considerations on the structure and the index of DAE obtained from the inverse bond graph to establish the need for a fresh approach. Section 4 then provides this fresh approach and presents the proposed configuration for performance specification system in series with actual inverse system for simulation. Conditions on specification system for the overall simulated system to be proper are studied in a structural point of view in simple cases and they can be extended to non-linear and complex systems. Section 5 illustrates the proposed method using the example of a two-arm robot and Section 6 concludes the paper.

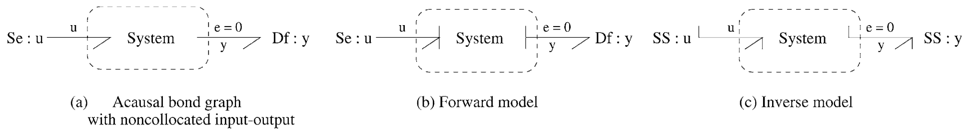

Fig. 1. Forward and inverse bond graph in the general case.

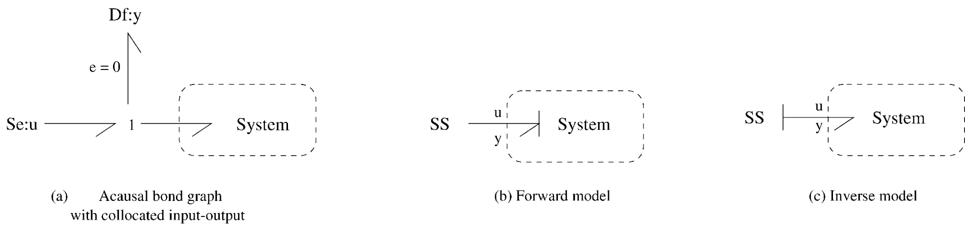

Fig. 2. Forward and inverse bond graph for collocated input–output.

2. Bond graph representation of the inverse model

An *acausal* bond graph model of a system is a graphical representation of the system which is independent of the particular computational problem that may interest the modeller; such problems include system analysis, simulation, system inversion, state estimation or parameter identification. Each of these problems can be considered in the bond graph context by augmenting the acausal bond graph with causal strokes which graphically represent the particular computational or mathematical problem to be solved. Causality assignment procedures for analysis and simulation of forward models (i.e. models describing the physical outputs and states in terms of inputs) are well-known [11–14].

More recently, bond graph representation of *inverse* models and some other problems mentioned above were considered using the concept of *bicausality* [15–17] where additional bond graph elements were introduced to enable this extended concept of causality to be used. These additional elements are described in Appendix A for completeness.

The general configuration proposed for a bond graph inverse model is shown in Fig. 1 where for the purpose of the example an effort associated to the **Se** element is the input and a flow measured by the **Df** element (flow detector) is the output. In the particular case of collocated input–output variables (i.e. when input and output are power variables associated to the same bond), it can easily be shown that the inverse model is obtained by reversing the causality of the corresponding **SS** element (Fig. 2).

A Sequential Causality Assignment Procedure for Inversion (SCAPI) that leads to an appropriate representation of inverse bond graph models was proposed in the case of SISO systems first and then extended to MIMO square systems [2,18].

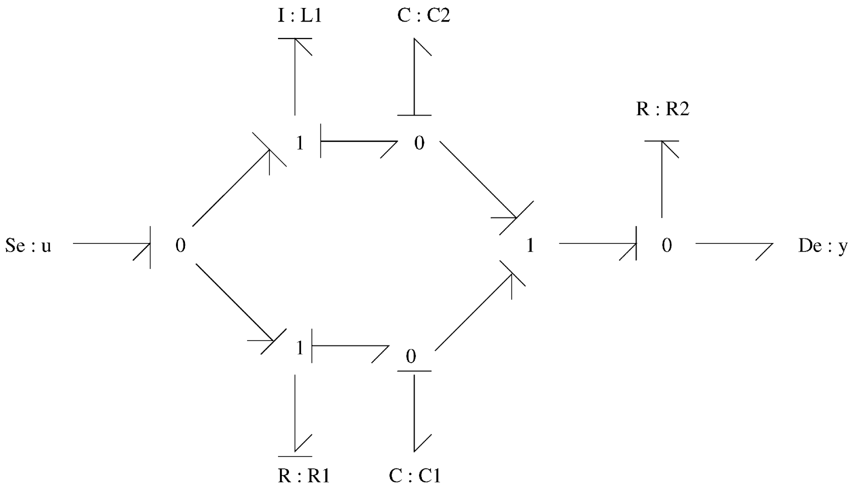

Fig. 3. Model with multiple input–output path.

This bond graph-based inversion procedure can be summarised into the three steps given below:

(1) In the forward model, determination of a minimal-order set of disjoint input–output causal paths or simply the minimal-order input–output path in the SISO case. The order of a causal path is defined as the difference between the number of elements in integral causality and the number of elements in derivative causality met on the considered path.
(2) Propagation of bicausal information from the output **SS** elements to the corresponding input **SS** elements through the previously determined minimal-order set of disjoint input–output causal paths and extension of their causal implications.
(3) Causal completion of the bond graph using classical causality assignment rules.

In fact, a bond graph in preferential integral causality is usually viewed as an appropriate model for the generation of equations associated with a specific problem. Causality assignment is then performed with the objective of maximising the number of storage elements in integral causality after the constraint causalities defining the problem have been assigned. Steps (1) and (2) of the procedure described above indeed give the maximal integral causality condition in the context of system inversion. For illustration, we consider the system given in Fig. 3. To represent its inverse model from the acausal bond graph, there are two possible ways to propagate the output–input bicausal information (Fig. 4a and b) giving two possible causal representations. The analysis of the input–output paths in the forward model gives the appropriate inverse model (Fig. 4b) without the need to try all possible causal configurations.

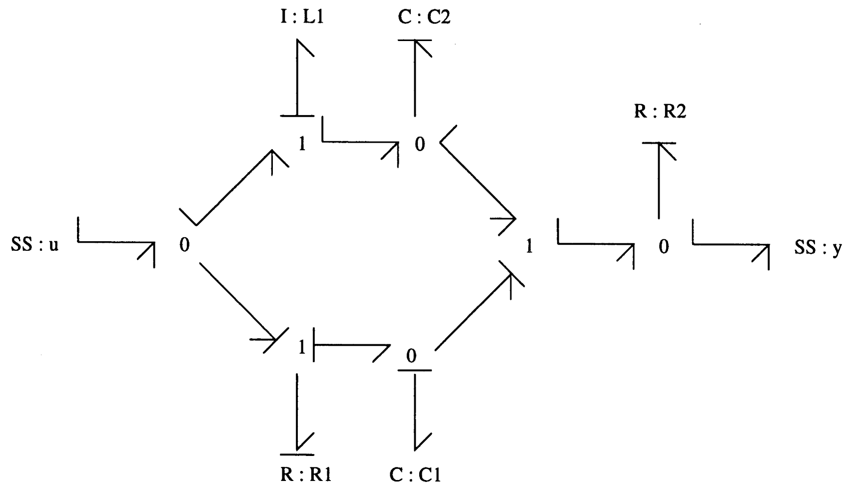

(a)

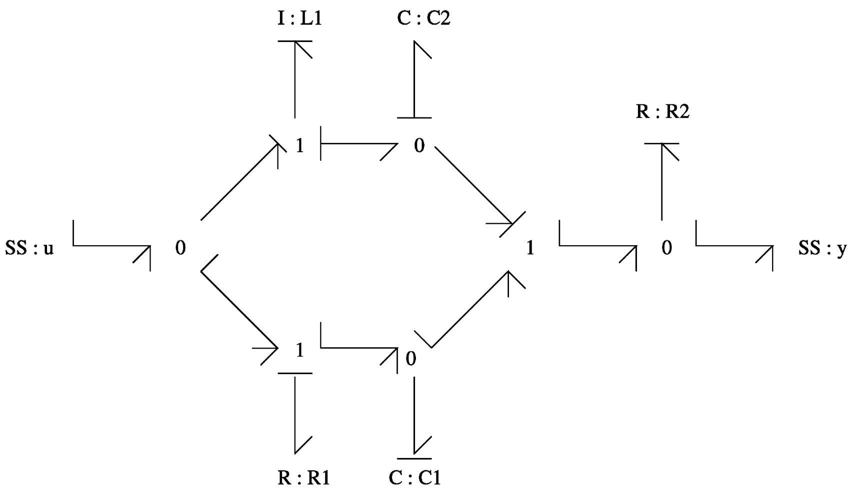

(b)

Fig. 4. Possible inverse model causal configurations.

3. Structure and equation form of the inverse model

The forward bond graph model of a system provides some indications on the structure of the associated DAE form by analysing the topological loops or zero-order causal paths in the model [19,20]. Direct coupling between input variables and dependent storage elements (that is in derivative causality) gives rise to consideration of the appropriateness of a physical model as it indicates that time derivative operations which are non-causal and thus, non-physically realizable operations may

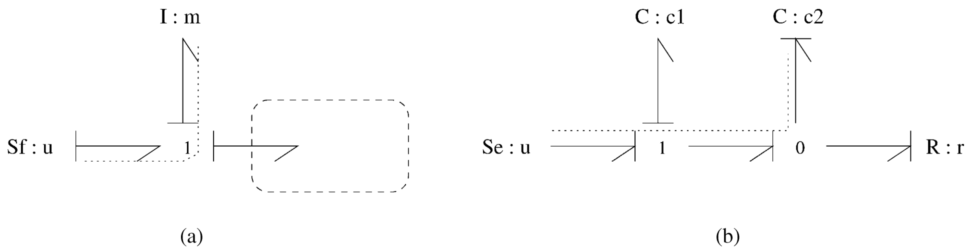

Fig. 5. Systems with direct coupling between input and dependent element.

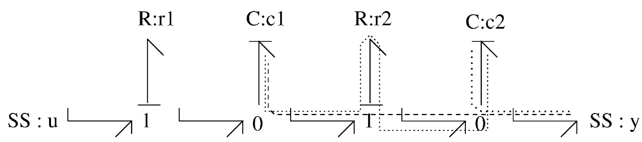

Fig. 6. Inverse model of a double RC-circuit.

be necessary to solve for the time evolution of the system in response to a given input [20,21]. In addition, direct coupling of two dependent storage elements is meaningless in a forward model as it is always possible to reverse their causality to obtain two storage elements in integral causality.

An example of such a system is shown in Fig. 5(a) where an equation of the form $\dot{p} = m\dot{u}$ exists in the state model which implies that the flow source **Sf** can instantaneously transmit any amount of power at any frequency to the **I**-element. Furthermore, writing the state equation of the system in Fig. 5(b) where there is a direct coupling between the input u and the dependent capacitive **C**:$c2$ gives the state equation (1) which is non-causal because of the time derivative of the input variable u. Therefore, such models cannot correspond to physically realisable systems.

$$\dot{q}_1 = -\frac{1}{r(c_1 + c_2)} q_1 + \frac{c_1 c_2}{(c_1 + c_2)} \dot{u}. \tag{1}$$

However, direct coupling between input variables and dependent storage elements on the one hand, and between dependent storage elements on the other will naturally appear in the inverse bond graph model due to the propagation of bicausality through the junction structure as bicausal bonds always have a strong causality on either 0 or 1 junctions. In this context such storage elements in derivative causality expressed the successive output derivatives required in the inverse model ODE form, they are not involved in zero-order causal loops and techniques commonly used to break the causal loops cannot be applied. The bond graph shown in Fig. 6 for example represents the inverse model of a double RC-circuit where there are direct couplings between y and $c1$, y and $c2$ and between $c1$ and $c2$. The DAE form of the inverse model is given by

$$\begin{aligned} q_1 &= c_1(\dot{q}_2 r_2 + y),\\ q_2 &= c_2 y, \\ u &= \dot{q}_1 r_1 + \dot{q}_2 r_1 + \dot{q}_2 r_2 + y. \end{aligned} \tag{2}$$

As there is no state in that model, the ODE form or minimal-order inverse equation (3) is an algebraic equation giving u in terms of y and its derivatives.

$$u = r_1 c_1 r_2 c_2 \ddot{y} + (r_1 c_1 + r_2 c_2)\dot{y} + y. \tag{3}$$

Alternatively, defining the *descriptor vector* X as

$$X = \begin{pmatrix} q_1 \\ q_2 \\ \dot{q}_1 \\ \dot{q}_2 \end{pmatrix}. \tag{4}$$

These equations can be rewritten as

$$\begin{aligned} E\dot{X} &= AX + Bu,\\ y &= CX + Du, \end{aligned} \tag{5}$$

where

$$E = \begin{pmatrix} 1 & 0 & 0 & 0 \\ 0 & 1 & 0 & 0 \\ 0 & 0 & 0 & 0 \\ 0 & 0 & 0 & 0 \end{pmatrix}, \tag{6}$$

$$A = \begin{pmatrix} 0 & 0 & 1 & 0 \\ 0 & 0 & 0 & 1 \\ -1 & 0 & 0 & c_1 r_2 \\ 0 & -1 & 0 & 0 \end{pmatrix}, \tag{7}$$

$$B = \begin{pmatrix} 0 \\ 0 \\ c_1 \\ c_2 \end{pmatrix}, \tag{8}$$

$$C = (0 \quad 0 \quad r_1 \quad r_1 + r_2), \tag{9}$$

$$D = (1). \tag{10}$$

The transfer function of this inverse system is then

$$G(s) = (\dot{C}(sE - A))^{-1}B + D = s^2 + (r_1 c_1 + r_2 c_2)s + r_1 c_1 r_2 c_2, \tag{11}$$

which is clearly not proper and thus, as expected, is not physically realizable. Although we have used a linear example here for clarity, the same conclusion arises for non-linear systems. The analysis and simulation of non-linear improper systems is not straightforward. For this reason, Section 4 provides an approach which avoids improper systems in this context.

4. Specification-based inversion

This section considers the problem of finding the input to a system that will make that system have the same output as another physical system (the specification system) driven by input such as a step function. It should be noted that only the determination of the input control function is of interest here and not the design of the controller that will achieve the output objective.

In the sequel, the specified physical system will be called *the specification system*. This specification system can be seen as a dynamic system (with possibly a bond graph representation) that generates the desired reference output trajectory which, when applied to the inverse of the actual system, will determine the required input function. The specification system must have appropriate structural dynamic properties, in particular, to ensure a realizable control signal the relative degree ρ_s of the specification system should be at least equal to the relative degree ρ of the actual system:

$$\rho_s \geqslant \rho. \tag{12}$$

One convenient and physically meaningful way to achieve this is to choose a specification system of the same physical structure (same bond graph model) as the actual system, but with parameters corresponding to desired performance.

In the case of *linear* systems, the required system input can, in principle, be found as the output of the system represented by the product of the transfer function of the specification system and the inverse transfer function of the system itself. However, such a transfer function representation is not available for non-linear systems and, even in the case of linear systems, loses the advantages of the bond graph representation such as showing the structure of the specification and the actual system and the possibility of carrying out some structural analysis on the global model using bond graph causality concepts. Therefore a bond graph based appoach is developed here.

Within the bond graph context, the above described operation of assembling the specification system in series with the inverse system (without reaction of the second system on the first one) cannot be achieved only with power bonds and conventional causality. This paper presents two distinct, but related, solutions to this problem, each using a non-standard connection components (see Appendix A) with potentially bicausal ports. These components are:

(1) amplifier **AE** and **AF** [22] components and
(2) zero **SS** [22,14] components imposing both zero effort and zero flow.

These two approaches are presented in Sections 4.1 and 4.2.

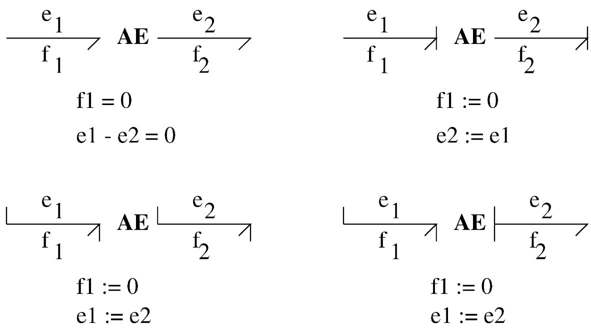

Fig. 7. Model and possible causal configurations of the AE-element.

4.1. Connecting with amplifier components

Although assembling systems without interaction can be done using signal bonds (also called active bonds) for interconnection, the resulting bond graph model cannot be used in the bicausal context as bicausal signal bonds cannot be readily represented [15]. For this reason, an alternative representation of signal bonds which preserves the uniformity of the bond graph representation can be obtained by considering that a signal bond is a particular case of power bond with one of the two associated power variables negligible and thus set to zero. Two new elements **AE** and **AF** whose constitutive relationships constrain the input power to be zero have been discussed by Gawthrop and Smith [22]. The detailed model and possible causal configurations of the **AE** element (effort amplifier) are shown in Fig. 7 and a dual model can be deduced for the **AF** element. The key idea is that the two effort variables are equal and independent of the flows and that the input flow variable is always zero—thus giving zero input power.

The difficulty of assembling systems in series with no mutual interaction using conventional bond graph is inherent to the conventional concept of causality. However, the extension of this concept to *bicausality* enables the decoupling of connected systems so that the non-reaction of the second system on the first one can be modelled.

As far as bond graph is used for analysis and simulation of forward models (i.e. time evolution of states and outputs in terms of given inputs), in the case of automated processing, there is almost no need for the user to specify some causalities in the model and all computations and analysis can be carried out automatically from the rough acausal model by the computer. But if it is admitted that the acausal bond graph model is a core representation for consideration of various problems such as estimation, identification or inversion, then it would be necessary to indicate on the acausal model at least a minimal causal information that would be required by a processor to perform a complete causality assignment and to generate the corresponding mathematical model. In many cases, this will be done by assigning the appropriate causalities to the **SS** elements [14] which are the generalisation of classical sources (**Se** and **Sf**) and detectors or sensors (**De** and **Df**) for computation objectives.

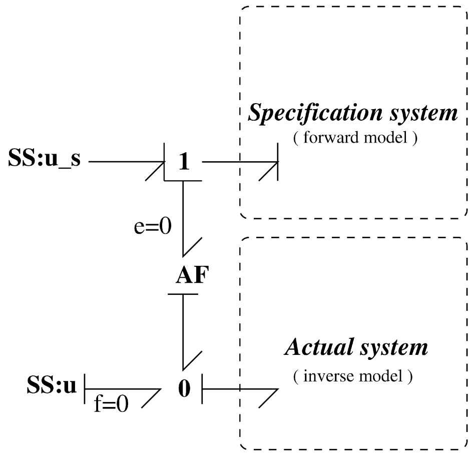

Fig. 8. Collocated input–output system.

Our purpose here is to propose a configuration model of the specification system assembled with the model of the actual system augmented with enough causal information in such a way that when a typical input is applied to the global system, its output is the required input to be applied to the actual system to obtain the performance specifications behaviour.

There are two cases to consider: collocated input/output pairs and non-collocated input output pairs. In each case, the issue is how to connect the system outputs together in such a way that the specification system is not affected by the connection.

Fig. 8 shows a system, and specification system, with *collocated* (effort) input and (flow) output joined by an **AF** component. The input to the specification system is imposed by the **SS** component labelled u_s, the corresponding flow is passed through the unit-gain **AF** component to provide the (flow) input to the inverse system. The **AF** component prevents interaction by imposing a zero effort at its input; the **SS** component labelled u provides a measurement of the inverse system (effort) output—the input that would make the system (effort) output behave as the specification system (effort) output.

Fig. 9 shows a system, and specification system, with *non-collocated* (effort) input and (effort) output. In this case, we regard the output of each system as being equipped with an **AE** component to isolate the system from flows at the output. The outputs of these **AE** components are directly connected via a junction, but with power flow directions as shown. The input port of the lower **AE** component is bicausal; not only does it impose the effort onto the output of the system, but also imposes the zero flow. This provides a very natural explanation of the known result that the inversion of systems with non-collocated input and output requires bicausal bonds.

The bicausal bond associated with the **SS** component labelled u carries not only the effort required to make the system behave as the specification system but also the corresponding covariable—thus the actuation *power* can also be deduced.

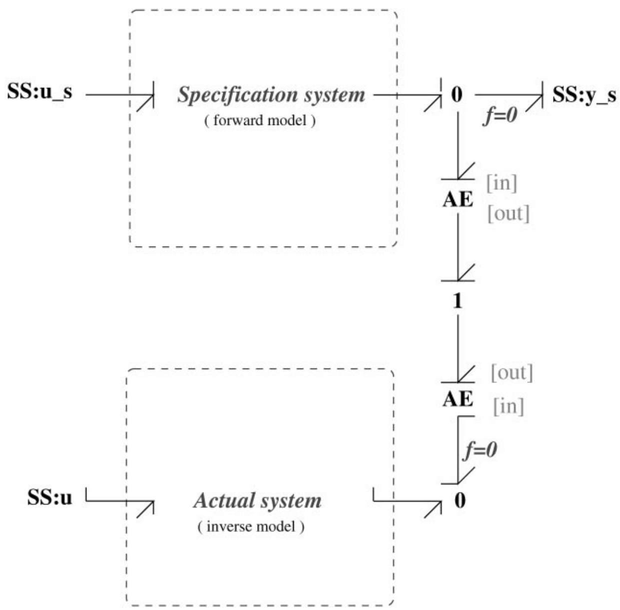

Fig. 9. Non-collocated input–output system.

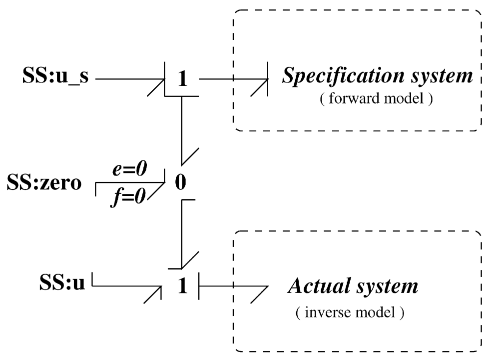

Fig. 10. Collocated system.

4.2. Connecting with zero **SS** components

An alternative to using **AE** and **AF** components is to provide the isolation of the specification system and inverse system using bicausal **SS** components imposing both zero effort and zero flow. As before, there are two cases to consider: collocated input/output pairs and non-collocated input/output pairs.

Fig. 10 shows a system, and specification system, with *collocated* (effort) input and (flow) output, acting on **1** junctions appearing at the system ports. These two **1** junctions are then connected via a **0** junction which also carries the **SS** component

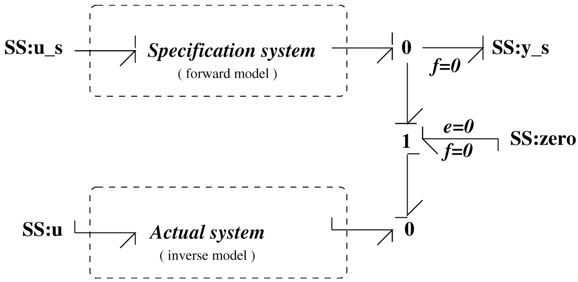

Fig. 11. Non-collocated system.

which imposes zero effort on both the **1** junctions thus providing the required isolation. In addition, the **SS** component imposes zero flow, thus ensuring that the output flow of the specification system passes unchanged to the inverse system.

Fig. 11 shows a system, and specification system, with *non-collocated* (effort) input and (effort) output. As before, the **SS** component labelled zero provides the required isolation. As before, this implies that the inverse system requires bicausal bonds.

Once again, in both the collocated and non-collocated cases, the bicausal bond associated with the **SS** component labelled u carries not only the effort required to make the system behave as the specification system but also the corresponding covariable—thus the actuation *power* can also be deduced.

5. Examples

This section contains two illustrative examples covering the range of systems considered in the paper:

- a linear, single-input–single-output non-collocated electrical system using the zero **SS** method and
- a non-linear two-input–two-output collocated mechanical system using the **AEAF** approach.

In each case the specification system is a physical system; in the first case it is the same physical system but with different parameters and in the second case it is a different physical system but with the same relative degree $\rho_s = \rho$.

In each case, the resultant composite (specification and inverse) system is proper and has an ordinary differential equation representation amenable to standard simulation techniques.

5.1. An RC electrical circuit

The bond graph of a two-stage RC circuit appears in Fig. 12. Causal strokes have been added to make clear the flow of causality through the actual system and

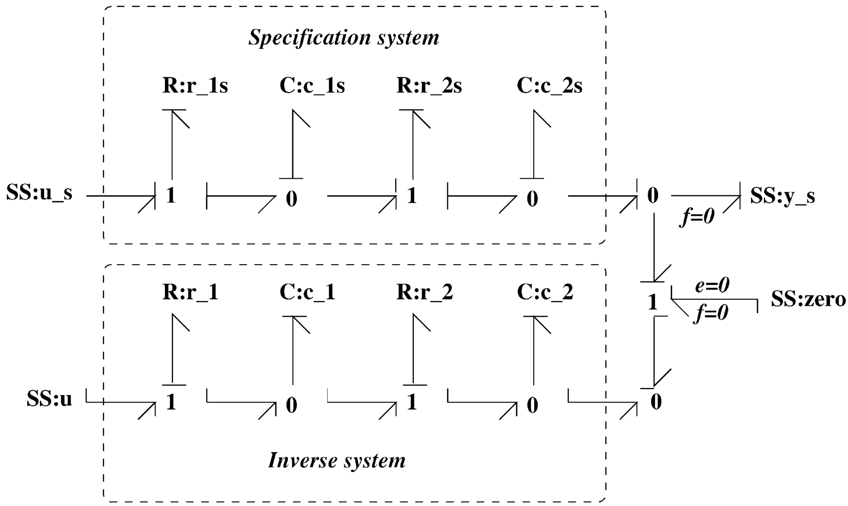

Fig. 12. An RC electrical circuit: bond graph.

specification system. This figure corresponds to the configuration proposed in Fig. 11. This composite system is linear and proper and can therefore be expressed in state-space form as

$$A = \begin{pmatrix} \dfrac{(-(r_{1s} + r_{2s}))}{(c_{1s}r_{1s}r_{2s})} & \dfrac{1}{(c_{2s}r_{2s})} \\ \dfrac{1}{(c_{1s}r_{2s})} & \dfrac{(-1)}{(c_{2s}r_{2s})} \end{pmatrix}, \tag{13}$$

$$B = \begin{pmatrix} \dfrac{1}{r_{1s}} \\ 0 \end{pmatrix}, \tag{14}$$

$$C = \begin{pmatrix} 0 & \dfrac{1}{c_{2s}} \\ \dfrac{(2((r_1 + r_2)c_2 + c_1 r_1))}{(c_{1s}c_{2s}r_{2s})} & \dfrac{(-(2c_1 r_1 - c_{2s}r_{2s} + 2(r_1 + r_2)c_2))}{(c_{2s}^2 r_{2s})} \\ \dfrac{(2(c_1 + c_2))}{(c_{1s}c_{2s}r_{2s})} & \dfrac{(-2(c_1 + c_2))}{(c_{2s}^2 r_{2s})} \end{pmatrix}, \tag{15}$$

$$D = (0). \tag{16}$$

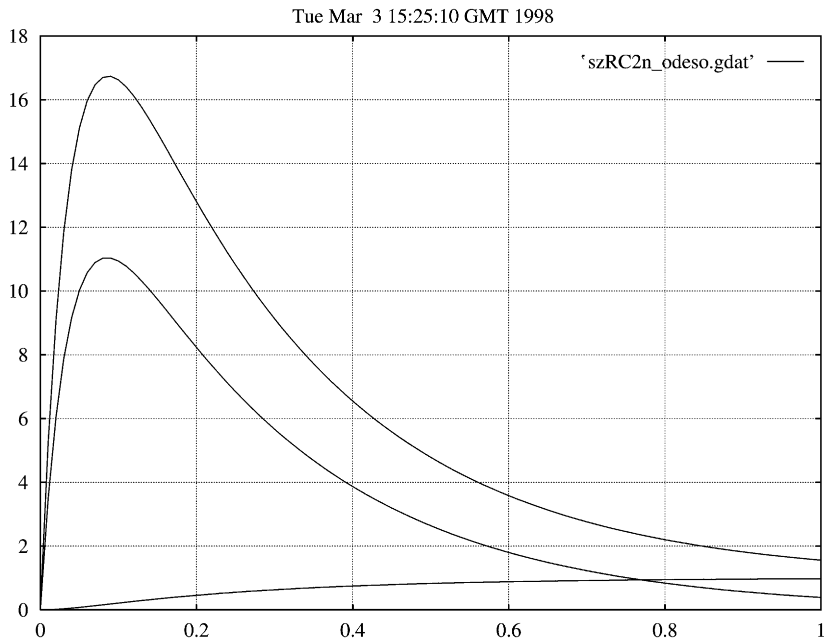

Fig. 13. An RC electrical circuit: step response.

For the purposes of exposition, the composite system has three outputs:

(1) the output y_s of the specification system which is in fact the desired output of the actual system, and
(2) the corresponding effort and flow at the system input (inverse system output)

These latter variables provide the information required for actuator sizing: effort, flow and power [2,18].

All physical parameters were set equal to one, except for the parameters of the two C components of the specification system which were set to $c_{1s} = c_{2s} = 0.1$. Thus, the specification system is "faster" than the system itself.

Fig. 13 shows the unit step response of this composite system; the lower graph corresponds to the output of the specification system; the other two graphs give the corresponding system input effort and flow variables. Fig. 14 shows the log magnitude of the composite system frequency response magnitude against log frequency; the three plots correspond to those of Fig. 13.

5.2. A two-link manipulator

Let us consider the problem of computing the torques to apply to the joints of a two-link manipulator so that each link behaves like a specified mass–spring–damper

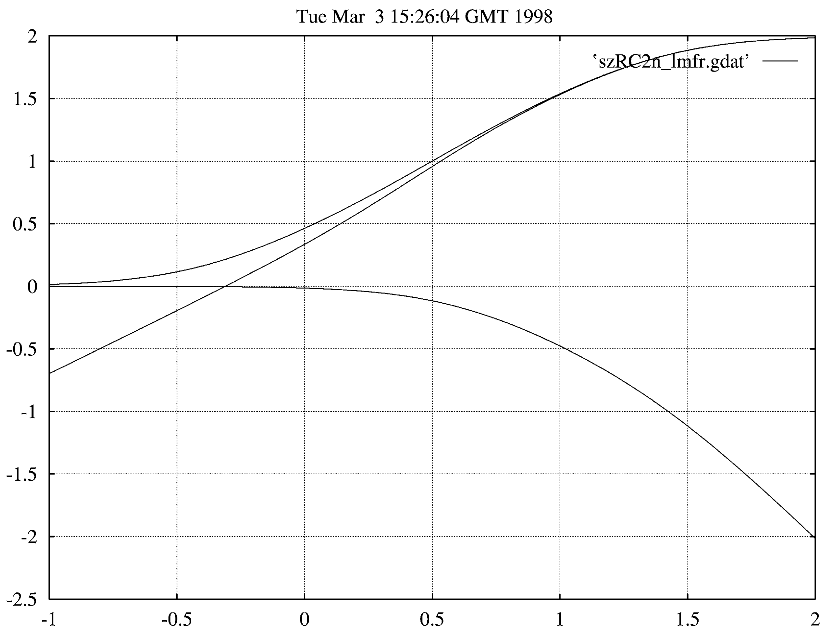

Fig. 14. An RC electrical circuit: frequency response.

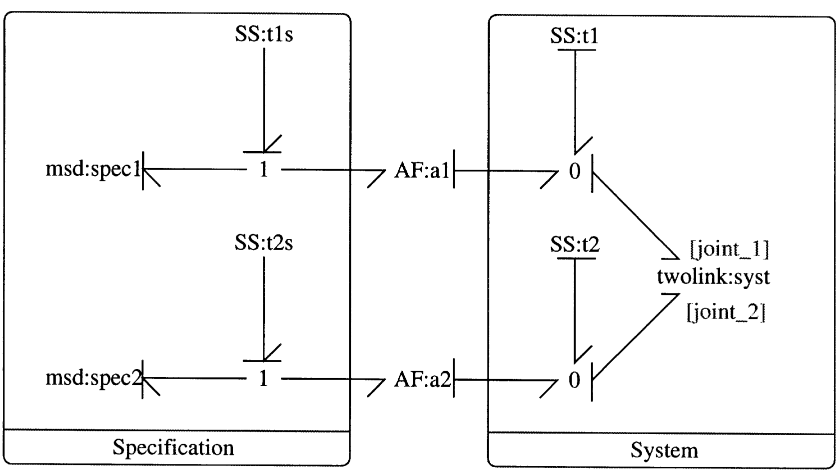

Fig. 15. A two-link manipulator: bond graph.

(msd) system in terms of time evolution of the angular velocity response to a step input.

In the bond graph model of the manipulator, torque and angular velocity of each joint are collocated variables and the global system configuration to model the

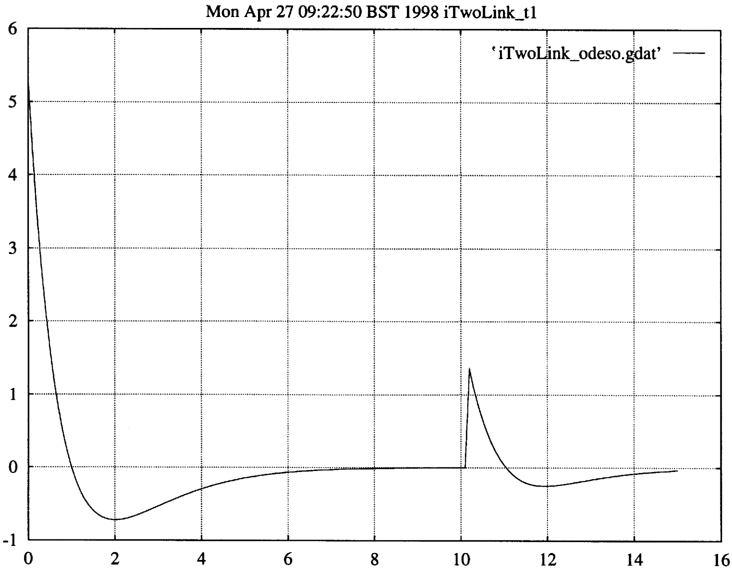

Fig. 16. A two-link manipulator: computed torque for port 1.

problem is shown in Fig. 15 where t1s and t2s are step inputs and t1 and t2 are the torque to be computed. This corresponds to the configuration proposed in Fig. 8.

The detailed models of subsystems msd and twolink are given in Appendix B.

The composite nonlinear system was simulated as follows. The manipulator consists of two unit length, unit mass, uniform rods in the horizontal plane driven by ideal torque sources at each joint. The corresponding outputs are the two joint angular velocities. Each specification system has unit mass, unit compliance and critical damping. The inputs to the specification system are each unit steps but that for the first joint starts at $t = 0$ and that for the second at $t = 10$. These inputs correspond to a one radian change in joint angle.

The computed torque for the first joint appears in Fig. 16 and that for the second joint in Fig. 17. As the corresponding velocities are also outputs of the simulation (not shown here), all of the information for actuator sizing (effort, flow and power) is thus available as a function of time. Conventionally, this information would be plotted on an effort/flow diagram superimposed on the allowable effort, flow and power curves for the possible actuators allowing an appropriate actuator type and size to be chosen.

6. Conclusion

The paper has shown that a *specification* system and an *inverse* system can be combined to give a physically realisable system inverse which can be represented by an ordinary differential equation and thus readily solved for use in, for example,

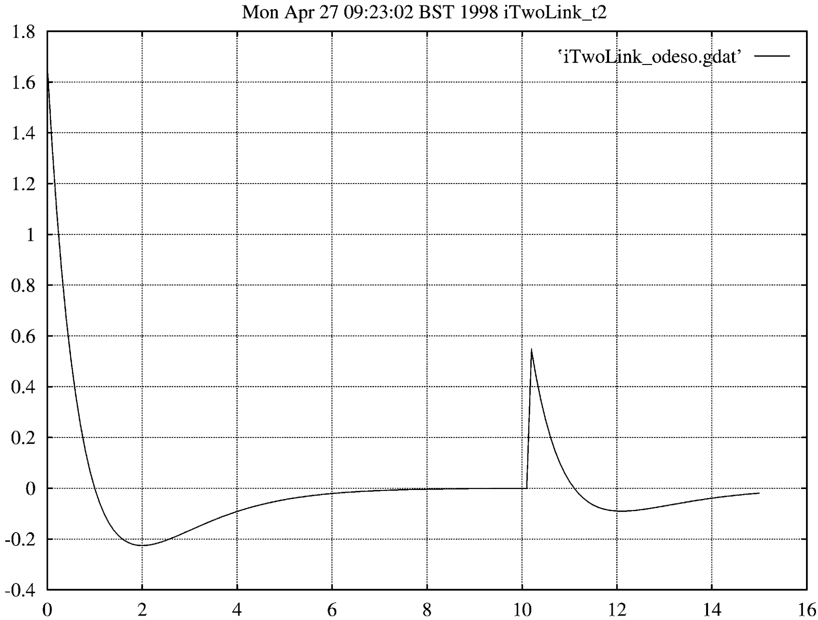

Fig. 17. A two-link manipulator: computed torque for port 2.

actuator sizing. This avoids the need for the differential-algebraic equation solution associated with standard methods of system inversion.

In the assembling of the *specification* system and the *inverse* system, the use of active bonds has been avoided in order to preserve computational possibilities associated with an acausal bond graph model. So, non-standard elements such as **SS**, **AE** and **AF** related to the concept of bicausality have been used enabling then to eventually consider other problems on the composite model simply by changing the causality assignment.

As the specification system is, itself a physical system corresponding to the ideal closed-loop system, we believe that this is another contribution to "Design in the Physical Domain" [23].

Appendix A. Non-standard bond graph elements

Non-standard bond graph elements presented here have been introduced to replace elements with imposed causality or some representations with active bonds for two main reasons:

(1) elements with imposed causality naturally set some limitations to the use of bicausality and the full exploitation of computational possibilities associated with bond graph models.

(2) active bonds constraint the orientation of variables and thus the causality in the model.

- **De and Df elements: effort sensor and flow sensor**

Elements used to indicate output variables in a bond graph model. These elements are defined so that the conjugate of the variable to be measured is set to zero.

Model with active bond	Model with **De** or **Df**	
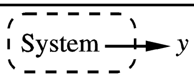	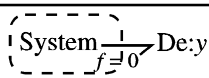	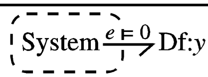

- **SS element: Source-Sensor**

Generic element used to replace **Se**, **Sf**, **De** and **Df** elements in bicausal bond graph. The nature of the SS element is then determined from the causality imposed by the problem under consideration. By default, **SS** elements will be used as input/output port elements of submodels.

Causal configuration	Nature of the **SS** element
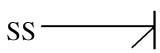	Effort source , flow sensor (**Se** element)
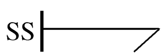	Flow source, effort sensor (**Sf** element)
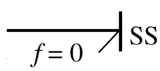	Zero flow source, effort sensor (**De** element)
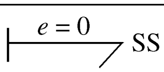	Zero effort source, flow sensor (**Df** element)
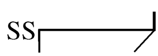	Flow source, effort source
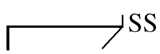	Flow sensor, effort sensor

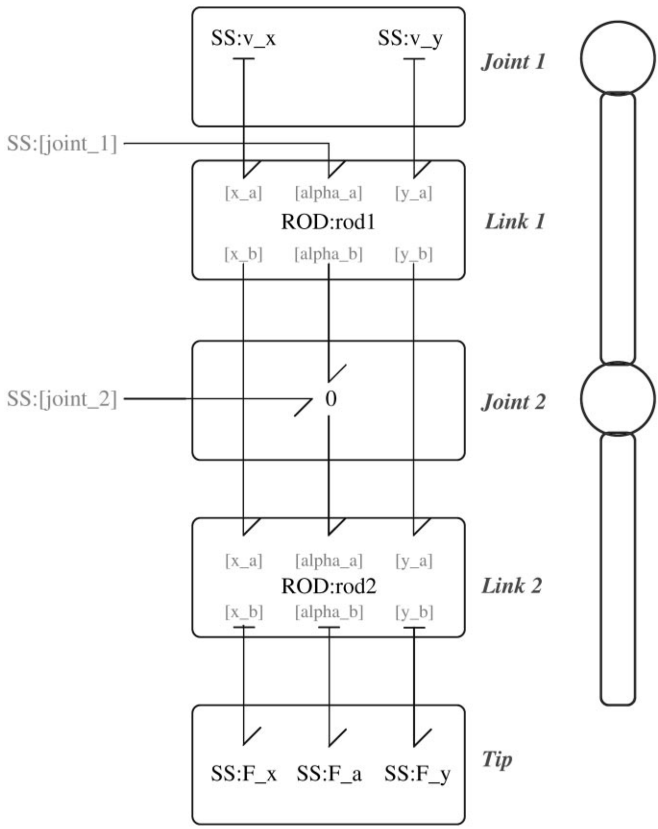

Fig. 18. Bond graph model of the twolink manipulator.

- **AE and AF elements: effort amplifier and flow amplifier**

Classical representations of amplifiers are modulated effort or flow sources. However, because of the reasons stated before, the new **AE** and **AF** elements are introduced here for the general case of k-gain effort amplifier. A dual model can easily be obtained for k-gain flow amplifier.

Acausal model	Causal configurations of **AE** element	
$\xrightarrow[f_1]{e_1}$ AE:k $\xrightarrow[f_2]{e_2}$ $f1 = 0$ $ke1 - e2 = 0$	$\xrightarrow[f_1]{e_1}$ AE:k $\xrightarrow[f_2]{e_2}$ $f1 := 0$ $e2 := ke1$	$\xrightarrow[f_1]{e_1}$ AE:k $\xrightarrow[f_2]{e_2}$ $f1 := 0$ $e1 := e2/k$

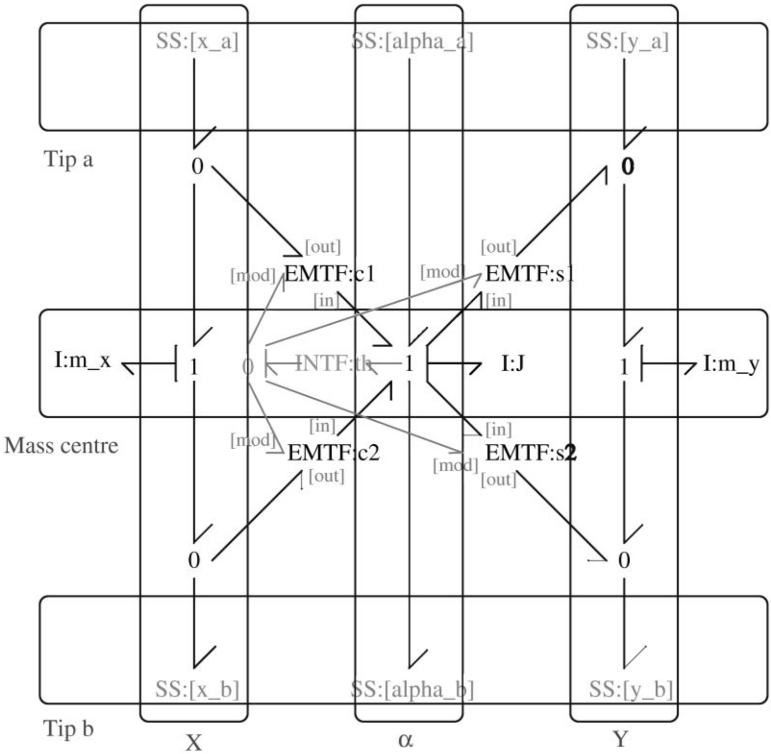

Fig. 19. Bond graph model a ROD.

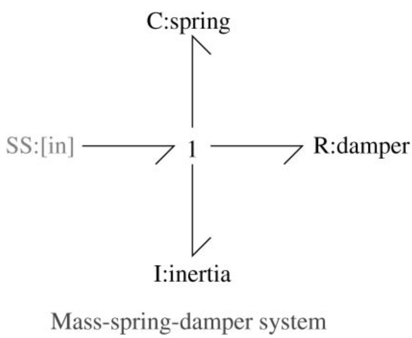

Fig. 20. Bond graph model of the msd specification.

- **INTE and INTF elements: integration/derivation of effort/flow**

These submodels are introduced as a substitution to classical block diagram representation of integral or derivative operations. Note that these models are to some extent close to electronical realization of integration with amplifiers. With unit gain amplifier and unit parameter **C**, integrations of flow or derivations of effort are obtained from causality assignment as shown below with **INTF** submodel. Dual representation can easily be obtained for **INTE** submodel.

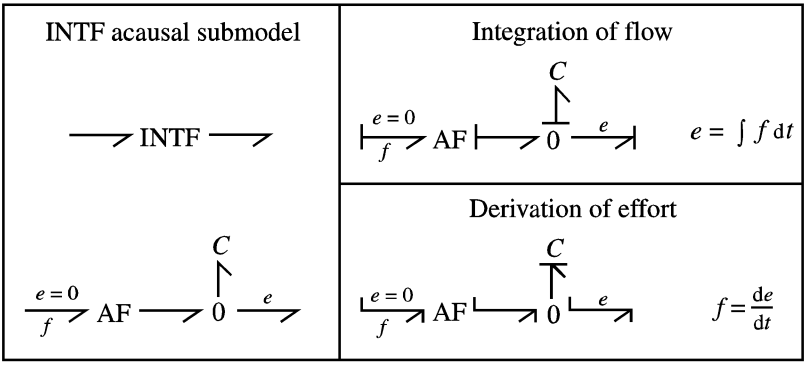

- **Miscellaneous: EMTF, FMTF, EMGY, FMGY, EMR, FMR,...**

These are classical modulated elements with a prefix **E** or **F** indicating the nature of the modulating variable.

Appendix B. Detailed models

The detailed models of the two-link manipulator and the mass–spring–damper specification presented in Section 5.2 are given in Figs. 18–20 by developing the bond graph models from a hierarchical word bond graph as described in Ref. [22].

References

[1] R.F. Ngwompo, Contribution au Dimensionnement des Systèms sur des Critères Dynamiques et Énergétiques—Approche par Bond Graph, Ph.D. Thesis, INSA de Lyon, 1997.
[2] R.F. Ngwompo, S. Scavarda, D. Thomasset, Inversion of linear time-invariant siso systems modelled by bond graph, J. Franklin Inst. 333 (B) (2) (1996) 157–174.
[3] C.W. Gear, L.R. Petzold, Ode methods for the solution of differential/algebraic systems, SIAM J. Numer. Anal. 21 (1984) 716–728.
[4] K.E. Brenan, S.L. Campbell, L.R. Petzold, Numerical Solution of Initial Value Problems in Differential-Algebraic Equations, North-Holland, New York, 1989.
[5] C.W. Gear, An introduction to numerical methods for odes and daes, in: NATO ASI Series, Vol. F69, Springer, Berlin, 1990, pp. 115–126.
[6] L.M. Silverman, Properties and application of inverse systems, IEEE Trans. Automat. Control 13 (1968) 436–437.
[7] H. Seraji, Minimal inversion, command matching and disturbance decoupling in multivariable systems, Int. J. Control 49 (6) (1989) 2093–2121.

[8] A. Isidori, Nonlinear Control Systems: An Introduction, 3rd Edition, Springer, New York, 1995.
[9] P.J. Gawthrop, H. Demircioglu, I. Siller-Alcala, Multivariable continuous-time generalised predictive control: a state-space approach to linear and non-linear systems, Proc. IEE Part D 145 (3) (1998) 241–250.
[10] H. Chen, F. Allgöwer, A quasi-infinite horizon non-linear model predictive control scheme with guarenteed stability, Automatica 34 (10) (1999) 1205–1217.
[11] D.C. Karnopp, D.L. Margolis, R.C. Rosenberg, System Dynamics: A Unified Approach, Wiley, New York, 1990.
[12] J.U. Thoma, Simulation by Bond Graphs, Springer, Berlin, 1990.
[13] J van Dijk. On the role of bond graph causality in modelling mechatronic systems, Ph.D. Thesis, Universitiet Twente, 1994.
[14] P.J. Gawthrop, L. Smith, Causal augmentation of bond graphs, J. Franklin Inst. 329 (2) (1992) 291–303.
[15] P.J. Gawthrop, Bicausal bond graphs, In: F.E. Cellier, J.J. Granda (Eds.), Proceedings of the 1995 International Conference on Bond Graph Modeling and Simulation (ICBGM'95), Simulation Series, Vol. 27, Las Vegas, USA, Society for Computer Simulation, January 1995, pp. 83–88.
[16] P.J. Gawthrop, Control system configuration: Inversion and bicausal bond graphs, in: J.J. Granda, G. Dauphin-Tanguy (Eds.), Proceedings of the 1997 International Conference on Bond Graph Modeling and Simulation (ICBGM'97), Simulation Series, Vol. 29, Phoenix, Arizona, USA, Society for Computer Simulation, pp. 97–102.
[17] P.J. Gawthrop, D.J. Ballance, Genevieve Dauphin-Tanguy. Controllability indicators from bond graphs, in: J.J. Granda, F. Cellier (Eds.), Proceedings of the 1999 International Conference on Bond Graph Modeling and Simulation (ICBGM'99), Simulation Series, Vol. 31, San Francisco, California, USA, Society for Computer Simulation, January 1999, pp. 359–364.
[18] R.F. Ngwompo, S. Scavarda, D. Thomasset, Structural invertibility and minimal inversion of multivariable linear systems—a bond graph approach, in: J.J. Granda, G. Dauphin-Tanguy (Eds.), Proceedings of the 1997 International Conference on Bond Graph Modeling and Simulation (ICBGM'97), Simulation Series, Vol. 29, Phoenix, Arizona, USA, Society for Computer Simulation, January 1997.
[19] J. van Dijk, P.C. Breedveld, Simulation of system models containing zero-order causal paths—i. classification of zero-order causal paths, J. Franklin Inst. 328 (5/6) (1991) 959–979.
[20] R.C. Rosenberg, State-space formulation for bond graph models of multiport systems, Trans. ASME 93 (1971) 35–40.
[21] N. Hogan, Modularity and causality in physical system modelling, Trans. ASME 109 (1987) 384–391.
[22] P.J. Gawthrop, L.P.S. Smith, Metamodelling: Bond Graphs and Dynamic Systems, Prentice-Hall, Hemel Hempstead, Herts, England, 1996.
[23] A. Sharon, N. Hogan, D.E. Hardt, Controller design in the physical domain, J. Franklin Inst. 328 (5) (1991) 697–721.